

Doppler-shifted Raman-Nath diffraction from gratings recorded in LiNbO₃ with ultra-short laser pulses of different color

Holger Badorreck,¹ Alexandr Shumelyuk,² Stefan Nolte,¹
Mirco Imlau¹ and Serguey Odoulov^{2,*}

¹*School of Physics, Osnabrück University, D-49076 Osnabrück, Germany*

²*Institute of Physics, National Academy of Sciences, 03 650 Kyiv, Ukraine*

[*odoulov@iop.kiev.ua](mailto:odoulov@iop.kiev.ua)

Abstract: Nominally undoped LiNbO₃ crystals feature a pronounced mixed (absorption/refraction) nonlinear response in the blue-green spectrum domain that is sufficient for the excitation of moving dynamic gratings and the observation of selfdiffraction with Doppler shifted higher orders. This type of Raman-Nath selfdiffraction can be successfully used for up- and down- frequency conversion as well as for characterization of the recording pulses.

© 2016 Optical Society of America

OCIS codes: (320.2250) Femtosecond phenomena; (090.0090) Holography.

References and links

1. M. Horowitz, B. Fischer, Y. Barad, and Y. Silberberg, "Photorefractive effect in a BaTiO₃ crystal at the 1.5- μ m wavelength regime by two-photon absorption," *Opt. Lett.* **21**, 1120–1122 (1996).
2. Hung-Te Hsieh, D. Psaltis, O. Beyer, D. Maxein, C. von Korff Schmising, K. Buse, and B. Sturman, "Femtosecond holography in lithium niobate crystals," *Opt. Lett.* **30**, 2233–2235 (2005).
3. A. Shumelyuk, M. Imlau, V. Dieckmann, H. Badorreck, A. Grabar, and S. Odoulov, "Self-diffraction from two-photon absorption gratings in Sn₂P₂S₆," *Opt. Lett.* **37**, 4065–4067 (2012).
4. S. Odoulov, A. Shumelyuk, H. Badorreck, S. Nolte, K.-M. Voit and M. Imlau, "Interference and holography with femtosecond laser pulses of different colours," *Nat. Commun.* 6:5866 doi: 10.1038/ncomms6866 (2015).
5. H. Crespo, J. T. Mendonca, and A. Dos Santos, "Cascaded highly nondegenerate four-wave-mixing phenomenon in transparent isotropic condensed media," *Opt. Lett.* **25**, 829–831 (2000).
6. J. L. Silva, R. Weigand, and H. M. Crespo, "Octave spanning spectra and pulse synthesis by nondegenerate cascaded four-wave mixing," *Opt. Lett.* **34**, 2489–2491 (2009).
7. Jinping He, Jun Liu, and Takayoshi Kobayashi, "Tunable multicolored femtosecond pulse generation using Cascaded Four-Wave Mixing in bulk materials," *Appl. Sci.* **4**, 444–467 (2014).
8. S. Cabuk and A. Mamedov, "A study of the LiNbO₃ and LiTaO₃ absorption edge," *Tr. J. of Physics* **22**, 41–45 (1986).
9. M. Sheik-Bahae, D. J. Hagan, and E. W. Van Stryland, "Dispersion and band-gap scaling of the electronic Kerr effect in solids associated with two-photon absorption," *Phys Rev. Lett.* **65**, 97–99 (1990).
10. H. Badorreck, S. Nolte, F. Freytag, P. Bäune, V. Dieckmann, and M. Imlau, "Scanning nonlinear absorption in lithium niobate over the time regime of small polaron formation," *Opt. Mat. Express* **5**, 2729–2741 (2015).
11. M. Imlau, V. Dieckmann, H. Badorreck, and A. Shumelyuk, "Tin hypophosphite: Nonlinear response in the sub-100 fs time domain," *Opt. Mater. Express* **1**, 953–951 (2011).
12. M. Imlau, H. Brüning, B. Schoke, R.-S. Hardt, D. Conradi, and C. Merschjann, "Hologram recording via spatial density modulation of Nb_{Li}^{4+/5+} antisites in lithium niobate," *Opt. Express* **19**, 15322–15238 (2011).
13. C. M. Cirloganu, L. A. Padilha, D. A. Fishman, S. Webster, D. J. Hagan, and E. W. Van Stryland, "Extremely nondegenerate two-photon absorption in direct-gap semiconductors," *Opt. Express* **19**, 22951–22960 (2011).
14. A. Fishman, C. M. Cirloganu, S. Webster, L. A. Padilha, M. Monroe, D. J. Hagan, and E. W. Van Stryland, "Sensitive mid-infrared detection in wide-gap semiconductors using extreme nondegenerate two-photon absorption," *Nat. Photonics* **5**, 561–565 (2011).

15. M. Imlau, H. Badorreck, and C. Merschjann, "Optical nonlinearities of small polarons in lithium niobate," *Appl. Phys. Rev.* **2**, 040606 (2015).
16. Pochi Yeh, "Two-Wave Mixing in Nonlinear Media," *IEEE J. Quant. Electron.* **25**, 484–519 (1989).
17. H.J. Eichler, P. Günter, and D. Pohl, *Laser-induced Dynamic Gratings*, Springer Series in Optical Sciences, vol. **50**, Springer Verlag, Berlin, Heidelberg, 1986.
18. R. Brubaker, Q. Wang, D. Nolte, E. Harmon, and M. Melloch, "Steady-state four-wave mixing in photorefractive quantum wells with femtosecond pulses," *J. Opt. Soc. Am. B* **11**, 1038–1044 (1994).
19. R. Trebino, *Frequency-Resolved Optical Gating: The Measurement of Ultrashort Laser Pulses* (Kluwer Academic Publishers, 2000).

1. Introduction

The experimental observation of Doppler-shifted selfdiffraction from a moving dynamic grating recorded in nominally undoped LiNbO₃ by beams with considerably different optical frequencies is described in this paper. The recording of holographic gratings, both permanent [1] and dynamic [2, 3] with ultrashort laser pulses in crystals like LiNbO₃ is not a new phenomenon. In majority of previous works the recording beams featured, however, identical spectra, i.e., the wave mixing was degenerate in frequency. The main difference of our approach is in the use of pulses with large frequency detuning Ω . As distinct from recently published results on permanent hologram recording with femtosecond pulses of different colors [4], a pronounced third-order nonlinearity of LiNbO₃ allows for creating of a grating that moves together with light fringes even if their velocity is comparable to the velocity of light.

A similar self-diffraction has been reported earlier for some glasses and crystals [5–7], where it was treated in terms of nonlinear optics as Cascaded Four Wave Mixing (CFWM) and nonlinear refraction responsible for wave coupling. Surprisingly, this effect was never reported, to our best knowledge, for well studied classical nonlinear crystal LiNbO₃, an important material in nonlinear photonics and widely used in ultrafast optical parametric oscillators/amplifiers. Our first aim is therefore to clarify what can be expected from LiNbO₃ in this respect. Here, pronounced two photon absorption (TPA) is involved in addition to nonlinear refraction. By choosing the recording photons with energy 2.5 eV, i.e., in the vicinity of 0.7 of band gap energy $E_g \approx 3.63$ eV [8] we come close to the wavelength range in which, according to the data of [9] the nonlinear refraction n_2 is expected to be considerably reduced (with the following change of its sign for larger frequencies). As a result, we do not observe the cascades of diffraction orders even in case of nearly ideal estimated phase matching conditions. At most, six additional beams become visible at ultimate intensities of the recording pulses, three with upshifted and three with downshifted frequencies. This can be explained by a mixed, absorption/refraction nonlinear response of LiNbO₃ in the green-blue spectral range, with relatively high contribution of two-photon absorption. Such explanation is confirmed by estimates of the diffraction efficiencies that can be expected with the known data on real and imaginary parts of $\chi^{(3)}$ susceptibility of our LiNbO₃ samples [10], obtained in z -scan measurements.

Our second aim is to show that the reported Raman-Nath selfdiffraction from a moving grating in LiNbO₃ provides a powerful tool of frequency conversion and can be used efficiently for the characterization of the recording pulses themselves (pulse duration, frequency chirp).

2. Experiment and discussion

A standard two-beam geometry of transmission grating recording is shown in Fig. 1. Two unexpanded recording beams with $\simeq 2.5$ mm spots are generated in two OPAs pumped by the same mode locked Ti:Sapphire laser; they consist of trains of $\simeq 120$ fs pulses with 1 kHz (or 1 Hz) repetition rate, the single pulse energy being in the range from 40 to 80 μ J. The major part of experimental results presented below are obtained with a fixed wavelength of one of the two pulses $\lambda_1 = 489$ nm (frequency $\omega_1 = 3.85 \times 10^{15}$ rad/s) and tunable wavelength of the other

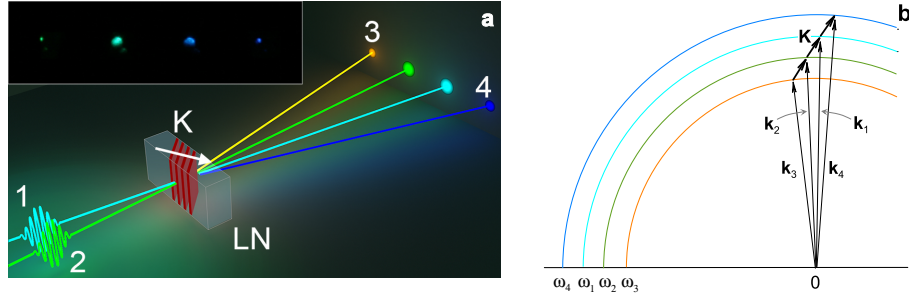


Fig. 1. (a) Experimental geometry: the incident beams 1 and 2 create a moving grating in the LiNbO₃ sample (LN), two diffracted beams 3 and 4 appear at the output in addition to transmitted beams 1 and 2. These beams form four colored spots in the far-field pattern shown in the upper left inset to this picture. (b) Schematic presentation of the wavevector diagram. The fragments of circles show the *xy*-crosssections of Ewald surfaces for the uniaxial crystal LiNbO₃, with radii equal to $k_i = \omega_i n_i / c$ for waves of different colors.

pulse. The description of the femtosecond laser system is given in [4, 11].

The plane parallel *y*-cut samples of nominally undoped LiNbO₃ (see for details [12]) have the polar axis *z* normal to the propagation plane of all beams, sample thickness being 200 μm. The electric field vectors of both recording beams are parallel to the crystal *z*-axis. The beams impinge upon the sample symmetrically, making in air ± 2° with respect to the normal of the input face. Most often the measurements are done with single fs pulses. For long term exposure of the sample in 1 Hz repetition rate operation mode no cumulative effects are observed. This allows for averaging over numerous consecutive pulses what is important in case of weak signals. With the described arrangement we observe quite pronounced self-diffraction into ± 1 diffraction orders (much weaker ± 2 and ± 3 orders can be seen for highest intensities of the recording beams). The far-field pattern (inset to Fig. 1) gives a representative example, with clearly visible diffraction spots; their spectra measured with Ocean Optics USB4000 spectrometer show obvious Doppler shifts.

The observed phenomenon can be interpreted as follows. Two waves with wavevectors $\mathbf{k}_1, \mathbf{k}_2$ and frequencies ω_1, ω_2 create a periodic dynamic fringe pattern with vector

$$\mathbf{K} = \mathbf{k}_1 - \mathbf{k}_2, \quad (1)$$

which is moving with velocity $v = \Omega / K$ (see, e.g., [4]). Here Ω is the frequency difference $\Omega = \omega_1 - \omega_2$ and K is the spatial frequency $K = |\mathbf{K}|$. In a medium with third order nonlinearity $\chi^3(\omega_1, \omega_1, \omega_2, -\omega_2) \neq 0$, moving fringes lead to the appearance of a moving grating of refractive index or two-photon absorption, or both. This grating can be revealed by the emerging additional waves with wavevectors $\mathbf{k}_3, \mathbf{k}_4$, which meet the phase matching conditions that are equivalent to the conditions of diffraction from a grating with grating vector \mathbf{K} (Eq. (1)):

$$\mathbf{k}_3 = \mathbf{k}_2 - \mathbf{K}, \quad \mathbf{k}_4 = \mathbf{k}_1 + \mathbf{K}, \quad (2)$$

what is shown in the wavevector diagram of Fig. 1(b). It should be underlined that both, the nonlinear index change and nonlinear absorption result from processes which are nondegenerate in frequency. They can, however, be comparably strong as degenerate process. It has been demonstrated convincingly in studies of extremely nondegenerate two-photon absorption in semiconductor crystals [13, 14].

As distinct from diffraction from a static grating, the diffraction from the moving grating

brings also changes in frequencies of diffracted waves,

$$\omega_3 = \omega_2 - \Omega, \quad \omega_4 = \omega_1 + \Omega, \quad (3)$$

what can be regarded as a consequence of the Doppler shift because of grating motion.

Figure 2(a) represents the experimentally measured frequencies of the twodiffracted waves as functions of frequency variation ω_2 for the fixed frequency $\omega_1 = 3.85 \times 10^{15}$ rad/s. Within the experimental error bars these dependences are linear and the measured data are close to straight lines, as plotted using Eq. (3). The dotted lines show a fixed frequency ω_1 of the recording beam 1, and adjustable frequency ω_2 of the recording beam 2.

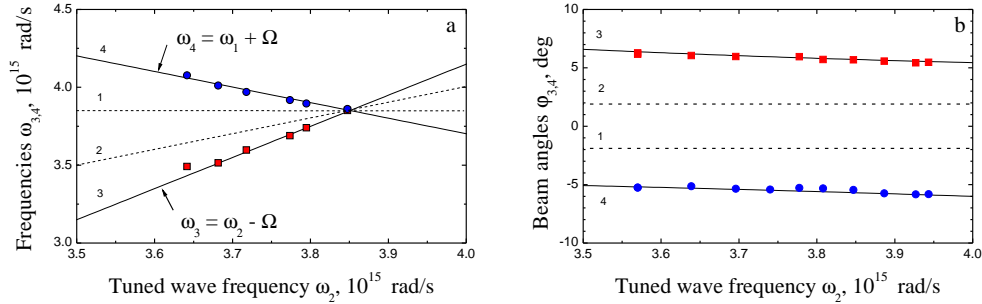


Fig. 2. Frequencies (a) and propagation angles (b) of four beams behind the sample versus frequency detuning of beam 2. Vertically polarized light beams impinge upon the 200 μm -thick y-cut LiNbO₃ plate in a plane parallel to the polar axis.

The propagation angles for the diffracted beams 3 and 4 can be found from Eq. (2). The calculated frequency detuning dependence of these angles are shown in Fig. 2(b) together with the experimental data. Once more, a satisfactory agreement of measured and calculated values can be stated. The dashed lines show fixed angles of the recording beams propagation.

For monochromatic cw waves that record a 3D grating the higher orders of diffraction are usually not phase matched and would not appear. For the recording with 120 fs pulses the restrictions imposed by phase matching are less rigid. Because of the relatively small effective thickness d the angular selectivity of the grating is rather poor and the tolerance $|\Delta\mathbf{K}| = 2\pi/d$ in meeting phase matching conditions of Eq. (2) is high. On the other hand, for transmission gratings with small spatial frequency (small angles between the recording beams) the spectral selectivity $\Delta\omega/\omega$ is quite soft, too, and covers transform limited temporal spectra of the recording pulses.

With the crystal dispersion taken into account, the calculations (see, e.g., Eq. (1) in [5]) show that nearly exact phase matching can be achieved for four consecutive diffraction orders with increasing temporal frequencies if the full crossing angle between the recording waves is reduced to 1° . This should result in the development of Cascaded FWM which was not observed, however, neither for 1° nor for other crossing angles. We believe it is a consequence of the large contribution of two-photon absorption to the recorded dynamic grating responsible for self-diffraction. A TPA grating with moderate contrast can produce by definition only ± 1 and ± 2 diffraction orders. On the other hand, the presence of TPA inhibits the grating which is due to the optical Kerr effect because it decreases the light intensity within the LiNbO₃ sample.

By using z -scan technique the nonlinear refraction constant n_2 and TPA coefficient β in samples cut from the same LiNbO₃ crystal have been estimated [11]. The measured values are $n_2 \approx 5 \times 10^{-20}$ m²/W and $\beta \approx 5.8$ mm/GW. The rough estimates of additive contributions to overall diffraction efficiency $\eta_{Kerr} \approx (\pi n_2 I_0 d / \lambda)^2$ and $\eta_{TPA} \approx (\beta I_0 d / 2)^2$ show that the contribution from the optical Kerr effect is much smaller than that from the nonlinear absorption

$\eta_{Kerr}/\eta_{TPA} \approx 0.01$. We want to note, that possible effects of free carriers and/or small polarons are not considered for the value of n_2 [15], which however does not change the presence of a mixed grating here.

We experimentally estimate also the conversion efficiency η of wave 2 into wave 3 (and 1 into 4). The values fall below 10^{-2} but they remain practically independent of the recording waves detuning within the range of $\Omega \approx 2 \cdot 10^{14}$ rad/s. It is known that any finite relaxation time of the nonlinear grating results in a diffracted intensity spectrum of Lorentzian type $\eta \propto [1/(1 + \Omega^2 \tau^2)]^2$ (see, e.g., [16]). Thus, a hypothetic inherent characteristic lifetime of the two-photon absorption grating at least much smaller than the reciprocal detuning range $1/\Omega$, i.e., $\tau_{TPA} \ll 5$ fs can be theoretically estimated.

3. Potential for pulse characterization

The dynamic gratings recording can be useful for the characterization of the recording pulses [17–19]. The four-wave mixing in photorefractive crystal has been successfully used to build a correlator that allows for estimating the femtosecond pulse duration [18]. We show that dynamic gratings in LiNbO₃ can be used for such measurements; they can provide in addition an information about the frequency chirp within the pulse, in a similar way as it is done in Rick Trebino’ FROG technique [19].

To perform such measurements the response of self-diffraction to a deliberately introduced time delay $\Delta t = t_1^0 - t_2^0$ between the recording pulses is studied (subscripts ”0” mark the pulse maxima). The time delay is controlled with an optical delay line in the recording beam 1 with larger frequency. Thus taking pulse 2 as a reference with $t_2^0 = 0$ we have positive Δt for delayed pulse 1. Figure 3 shows time delay dependences of diffracted orders intensities and frequencies.

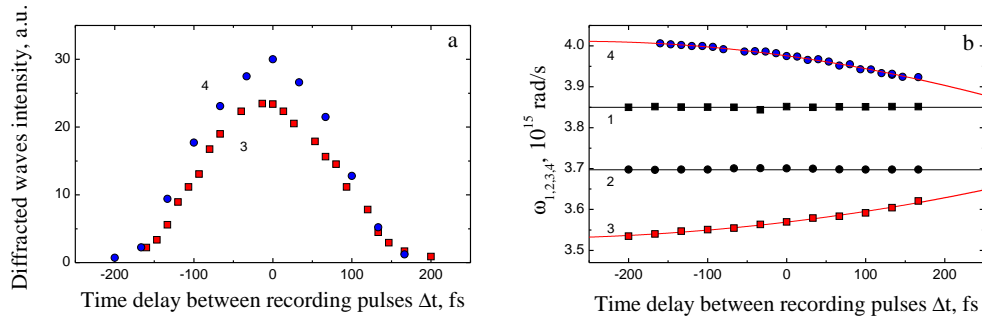


Fig. 3. Intensities (a) and spectral positions (b) of the diffracted pulses 3, 4 versus time delay between the recording pulses with the wavelengths $\lambda_1 = 489$ nm and $\lambda_2 = 509$ nm.

The characteristic bell shaped dependence of the intensity (Fig. 3(a)) reveals information about the pulse duration (see, e.g., [17–19]). For Gaussian shape of the recording pulses the FWHM of the diffraction efficiency should be $\sqrt{2}$ larger than the FWHM of the pulse itself [18].

The dependence of the diffracted beams frequencies on the mutual pulse delay proves that the instantaneous frequencies within the recording pulses change in time, i.e., pulses are chirped. Let’s consider that the central frequencies of the diffracted pulses 3,4 in Fig. 3(b) can be described by a Taylor series expansion up to second order:

$$\omega_{3,4}(\Delta t) = \omega_{3,4}(0) + \frac{d\omega_{3,4}}{d(\Delta t)} \cdot \Delta t + \frac{d^2\omega_{3,4}}{d(\Delta t)^2} \cdot (\Delta t)^2 + \dots \quad (4)$$

Here $d\omega/d(\Delta t)$ and $d^2\omega_{3,4}/d(\Delta t)^2$ are the linear and the second order pulse chirp components.

We assume, in first approximation, only a dominating linear chirp for the frequencies $\omega_1(t - \Delta t)$ and $\omega_2(t)$, the chirp being identical for both pulses because of their common origin. Then the frequency difference $\omega_1 - \omega_2$ is independent of the running time t for any arbitrary time delay Δt and remains constant during pulse propagation inside the sample. The higher orders of diffraction 4 and 3 will be upshifted and downshifted in frequency just for $\omega_1 - \omega_2$ which is a function of pulse delay Δt . This allows to deduce the relationship between the frequency difference of higher diffraction orders $\Omega_{4-3} = \omega_4 - \omega_3$ and the chirp parameter $d\omega/dt$ of the incident pulses 1,2

$$\frac{d\omega}{dt} = -\frac{1}{3} \frac{d\Omega_{4-3}}{d(\Delta t)} = -\frac{1}{3} \left(\frac{d\omega_4}{d(\Delta t)} - \frac{d\omega_3}{d(\Delta t)} \right). \quad (5)$$

The comparison of experimental data of Fig. 3(b) with the above considerations brings us to the conclusion that we are dealing with positively chirped pulses, $d\omega/dt > 0$. By extracting a linear term of a polynomial fit in Fig. 3(b) the absolute value of the linear chirp is estimated to be $d\omega/dt \simeq (0.16 \pm 0.02) \cdot 10^{27}$ rad/s². Taking the second order term in Eq. (4) into account, information on higher order chirp coefficients can be obtained, too. The chirp measured in this experiment is the inherent feature of the recording pulses themselves, it could be increased or partially compensated for by using two-grating pulse compressor.

In the limiting case of frequency degenerate recording beams, $\omega_1 = \omega_2$, the described technique is identical to the self-diffraction based implementation of FROG [19]. Working with recording pulses that are non-degenerate in frequency ensures an obvious advantage: the signal-to-noise ratio of the diffracted pulses can be largely improved by profiting from spectral filtering in addition to spatial (angular) filtering typical to all self-diffraction techniques. A single-shot variation of this technique is possible if traditional spectrometers with an input slit are used instead of the Ocean Optics spectrometer with small circular input aperture.

4. Summary and conclusions

The superposition of two pulses of different color in LiNbO₃ sample results in the appearance of Doppler-shifted diffracted beams, even in the spectral range of pronounced two-photon absorption. As a remarkable feature, the diffracted beams, upshifted and downshifted in frequency, are observed up to ± 3 order, however with no cascading to the higher diffraction orders. Using the language of transient gratings the phenomenon can be explained by the recording of a mixed nonlinear absorption and nonlinear refraction grating, that moves at a velocity close to the velocity of light. It becomes possible to explain the appearance of symmetric diffraction orders in \pm directions, to evaluate the diffraction efficiency and estimate, for the first time for LiNbO₃ the upper limit of the grating relaxation time to be less than 5 fs. Straightforwardly, the findings are applied for simple measurements of the chirp of incident recording beam.

Our results highlight the importance of two-photon absorption nonlinearity and explain the inhibition, in the used frequency range, of Cascaded FWM. It is not excluded, that the latter will emerge in the frequency range with negligible two-photon absorption, in the near infrared.

The described phenomenon is treated in terms of recording and self-diffraction from the dynamic grating which is moving with high velocity and brings therefore Doppler shift for diffracted waves. The purpose is not simply to introduce other language to the field; we are convinced that being extended to strongly nondegenerate interactions it will provide new important results in future, especially related to nonlinear coupling of beams with different colors.

Acknowledgments

Financial support of Deutsche Forschungsgemeinschaft, DFG (IM37/5-2, INST 190/137-1 FUGG, INST 190/165-1 FUGG) and Alexander von Humboldt Stiftung (S. Odoulov Research Award) is gratefully acknowledged. We thank Prof. Dr. Eckhard Krätzig and Dr. Javid Shirdel for fruitful discussions.